

The influence of $(n - n')$ -mixing processes in $He^*(n) + He(1s^2)$ collisions on $He^*(n)$ atoms' populations in weakly ionized helium plasmas

A. A. Mihajlov^a Lj. M. Ignjatović^{a,1} V. A. Srećković^a
Z. Djurić^b

^a*Institute of Physics, P.O.Box 57, Pregrevica 118, 11080 Zemun, Belgrade, Serbia*

^b*Silvaco Data Systems, Compass Point, St Ives PE27 5JL, UK*

Abstract

The results of semi-classical calculations of rate coefficients of $(n - n')$ -mixing processes due to collisions of Rydberg atoms $He^*(n)$ with $He(1s^2)$ atoms are presented. It is assumed that these processes are caused by the resonant energy exchange within the electron component of $He^*(n) + He$ collision system. The method is realized through the numerical simulation of the $(n - n')$ -mixing processes, and is applied for calculations of the corresponding rate coefficients. The calculations are performed for the principal quantum numbers n, n' in ranges $4 \leq n < n' \leq 10$, and the atom and electron temperatures, T_a, T_e , in domains $5000K \leq T_a \leq T_e \leq 20000K$. It is shown that the $(n - n')$ -mixing processes can significantly influence the populations of Rydberg atoms in non-equilibrium weakly ionized helium plasmas with ionization degree $\sim 10^{-4}$. Therefore, these processes have to be included in the appropriate models of such plasmas.

Key words: atomic and molecular collisions, Rydberg states

1 Introduction

Several existing models of collisional-radiative recombination [1–9] showed that in the weakly ionized plasmas, with ionization degree $\sim 10^{-4}$, the electron transfer from the lowest atomic states to the continuum and in the opposite direction is dominantly caused by the cascade mechanism. These processes of excitation/de-excitation are very important for populations in the lower part

¹ e-mail: ljuba@phy.bg.ac.yu

of the Rydberg's block of states. The reason for this is the distribution function of the excited atom states' populations in weakly ionized plasmas, which shows a distinct minimum ("bottleneck") in the lower part of Rydberg's block of states. For example, paper [10] compared LTE (local thermodynamical equilibrium) and non-LTE distribution functions, corresponding to different layers of the solar photosphere [5, 6]. It was found that both functions had distinct minimum in the domain of principal quantum numbers $n = 5 - 6$. Such behavior is illustrated in Fig. 1, showing LTE distribution functions for hydrogen plasmas at the temperatures $T = 5000K$ and $6000K$.

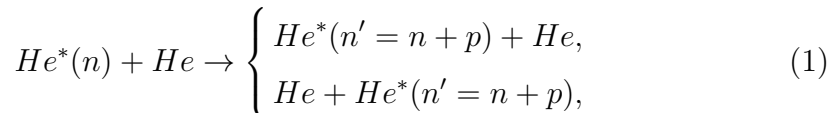
Similar behavior of the distribution functions for excited atomic states in the case of weakly ionized helium plasmas, for the temperatures $T = 10000K$ and $12000K$ typical for photospheres of some helium rich white dwarfs [11], is illustrated in the same figure. The experimental data for weakly ionized plasma of non equilibrium helium arc [12], show that the distribution function has a similar shape, even in the case when the electron temperature is four times higher than atomic temperature. It can be concluded that the kinetics of weakly ionized hydrogen and helium plasmas strongly depends on excitation and deexcitation processes in the region $4 \lesssim n \lesssim 10$, where the "bottleneck" of distribution function occurs.

The models of collisional-radiative recombination, used to estimate the influence of non-elastic processes which populate the lower part of Rydberg's block of states, included the radiation processes and the excitation/de-excitation processes caused by electron-atom collisions. The latter was assumed to be dominant for plasmas with the ionization degree $\sim 10^{-4}$. However, the distribution of excited atom states' populations experimentally obtained in [12], showed a significant influence of $(n - n')$ -mixing processes in $He^*(n) + He(1s^2)$ collisions. It was found that the distribution function was similar to Boltzmann with the temperature about $11000K$, close to the mid-value between $T_a \cong 4500K$ and $T_e \cong 18000K$. Consequently, the mechanism of the resonant energy exchange within the electron component of the atom-Rydberg atom collision systems (*resonant mechanism*) has been introduced in [13] to explain such a behavior. In cited paper and in [14, 15] the resonant mechanism was tested only for $(n - n')$ -mixing processes in $H^*(n) + H(1s)$ collisions, and the results obtained had only a qualitative character.

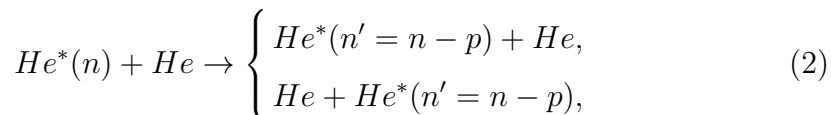
The resonant mechanism has been successfully applied to chemi-ionization processes in alkali Rydberg's atoms collisions with their parents' ground state [16], and further for alkali atoms' collisions [17-26]. In the case of hydrogen and helium atoms, the resonant mechanism was used to analyze the chemi-ionization and their inverse chemi-recombination processes [27-33]. It was shown that in weakly ionized hydrogen and helium plasmas the chemi-ionization/recombination processes caused by the resonant mechanism can be dominant in populating the Rydberg's states. This mechanism was also

investigated in the case of $(n - n')$ -mixing processes in $H^*(n) + H$ collisions populating the states within the Rydberg's block [10] (see also [14, 15]). In [10] the corresponding rate coefficients were determined as functions of n and T_a . It was shown that in hydrogen plasma with the ionization degree $\sim 10^{-4}$, and $4 \leq n \leq 10$, the efficiency of these processes is comparable or even higher than the concurrent excitation/de-excitation processes caused by electron-atom collisions. This was confirmed later for weakly ionized hydrogen plasma of solar photosphere in [34].

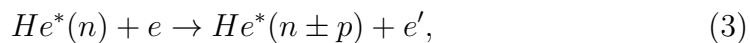
The efficiency of the resonant mechanism for chemi-ionization/recombination processes in weakly ionized hydrogen and helium plasmas [29, 30] suggested that one should expect similar situation in the case of $(n - n')$ -mixing processes. The semi-classical method based on this mechanism, developed in [10], was used in this paper and applied for the rate coefficients' calculations of excitation processes



and their inverse deexcitation processes



with $p \geq 1$. The processes are characterized by the excitation and deexcitation rate coefficients $K_{n;n+p}(T_a)$ and $K_{n;n-p}(T_a)$, respectively, where T_a is the atom temperature. They represent the average characteristics of transitions from all individual states with a given n to all states with given $n + p$ or $n - p$, and reflect the processes' influence on the plasma kinetics. The calculations are performed for the parameters' domains $4 \leq n \leq 10$, $1 \leq p \leq 5$ and $4000K \leq T_a \leq T_e \leq 20000K$. The efficiency of processes (1) and (2) is compared to the concurrent electron-excited atom collisional excitation/de-excitation processes



where e and e' denote free electron in the initial and final state, for given n , p and electron T_e .

Beside of processes (3) in the plasma occur the other concurrent processes, including the radiative processes caused by the interaction of excited atoms with the electromagnetic radiation. However, just the processes (3) are taken as referent ones since they are always included in the modeling of weakly ionized plasma disregarding to other concurrent processes. Consequently, in

order to demonstrate the necessity of including of the processes (1) and (2) in the models of weakly ionized plasmas, it is enough to show that their efficiency is comparable with the efficiency of processes (3).

2 Theoretical remarks

Resonant mechanism. The resonant mechanism of non-elastic $(n - n')$ -mixing and chemi-ionization/recombination processes in $A^*(n) + A$ collisions was described in details in previous papers [10, 14, 17, 27, 28]. In considered cases A was an atom in the ground state with one or two s -electrons out of completely filled shells. The mechanism, briefly described here, is illustrated by Fig. 2a and Fig. 2b.

Fig. 2a shows that the resonant mechanism's region is defined by the inequality

$$R \ll r_n, \quad (4)$$

where R is the internuclear distance and $r_n \sim n^2$ the characteristic radius of Rydberg's atom $A^*(n)$. In this region a perturbation operator takes the dipole part of the interaction between the outer electron e_n and the sub-system $A^+ + A$.

The electronic state of the $A^+ + A$ sub-system is described by the wave functions of the adiabatic ground ($|1; R\rangle$) and first excited ($|2; R\rangle$) electronic states of the molecular ion A_2^+ . The potential curves of these states are denoted with $U_1(R)$ and $U_2(R)$, and schematically shown in Fig. 2b. The impact energy of the collisional system, determined in the center of mass' system, is denoted with E . Fig. 2b illustrates that the resonant mechanism takes into account the transitions $|n\rangle \rightarrow |n+p\rangle$, $|n\rangle \rightarrow |\vec{k}\rangle$ and $|\vec{k}\rangle \rightarrow |n\rangle$, $|n\rangle \rightarrow |n-p\rangle$ of the outer electron, which occur simultaneously with the transitions $|2; R\rangle \rightarrow |1; R\rangle$ and $|1; R\rangle \rightarrow |2; R\rangle$ in the sub-system $A^+ + A$.

The main cause of the resonant character of described mechanism is the importance of transitions in the close vicinity of the corresponding resonant distances. In the case of $(n - n')$ -mixing, the resonant distances $R_{n;n\pm p}$ are found as roots of the equation

$$U_{12}(R) \equiv U_2(R) - U_1(R) = |\epsilon_{n\pm p} - \epsilon_n|, \quad (5)$$

where ϵ_n and $\epsilon_{n\pm p}$ denote electron energies in bound states with principal quantum numbers n and $n \pm p$. Note that for the chemi-ionization processes the resonant distances $R_{n;k}$ are found from (5) by replacing $\epsilon_{n\pm p}$ with the energy of the outer electron in free state, ϵ_k .

The described resonant mechanism for $(n - n')$ -mixing processes (1) and (2) is applied in helium case: $|1; R\rangle$ and $|2; R\rangle$ are $X^2\Sigma_u^+$ - and $A^2\Sigma_g^+$ -states of the molecular ion He_2^+ . The adiabatic potential curves $U_1(R)$ and $U_2(R)$ are taken from [35, 36]. The resonant distances $R_{n;n\pm p}$ are determined from Eq. (5) with these potential curves. The values of $R_{n;n+p}$ for $4 \leq n \leq 10$ and $1 \leq p \leq 5$ are presented in Table 1.

The rate coefficients' calculations require the quantity $D_{12}(R) = |\langle 1; R | \mathbf{D} | 2; R \rangle|$, where \mathbf{D} is the operator of the dipole momentum of the molecular ion He_2^+ . Table 1 shows that for all values of $R_{n;n+p}$ the inequality $R \gg a_0$ holds (a_0 being the atomic unit of length), and for D_{12} the approximation from [10] can be used

$$D_{12}(R) = \frac{e \cdot R}{2}, \quad (6)$$

where e is the absolute value of electron charge.

The method of calculations. $He^*(n \geq 4) + He$ and $H^*(n \geq 4) + H$ collision systems have similar behavior in $R \gg a_0$ region, which has been used for the chemi-ionization processes' calculations [30, 33]. On the other hand, the resonant mechanism generates transitions between Rydberg's states of outer electron that are allowed by selective rules. This was used to apply a semi-classical theory for the chemi-ionization processes in the cases of hydrogen [28, 29] and helium [30, 33].

The $(n - n')$ -mixing processes in $He^*(n) + He$ collisions are considered to be a result of the same resonant mechanism as in previous cases. The similarities between hydrogen and helium collisional systems made it possible to apply a semi-classical theory from [10] for processes (1) and (2). It means that the rate coefficients for these processes can be determined by the same procedure used in [10], but with the molecular ion He_2^+ characteristics instead. Consequently, the rate coefficients $K_{n;n+p}(T_a)$ for excitation processes (1) are determined directly, and the coefficients $K_{n;n-p}(T_a)$ for deexcitation processes (2) by using thermodynamical balance principle.

Similar to [10], the rate coefficients $K_{n;n+p}(T_a)$ are calculated under assumptions that:

- the internuclear motion occurs with the probability 1/2 in the potential $U_2(R)$ (molecular state $|2; R\rangle$), and can be described by the classical trajectory determined by the impact parameter and energy E ;
- the transitions $|2; R\rangle|n\rangle \rightarrow |1; R\rangle|n+p\rangle$ for $p = 1, 2, \dots$ happen continually along the trajectory, and are characterized by their rates;
- the atomic component has a Maxwell distribution described by the impact energies E with a given temperature T_a .

Applying the method from [10], the excitation rate coefficients $K_{n;n+p}(T_a)$ are

given as

$$K_{n;n+p}(T_a) = \frac{2\pi}{3\sqrt{3}} \frac{(ea_0)^2}{\hbar} \cdot n^{-5} \cdot g_{n;n+p} \times \int_{R_{min}(n,n+p)}^{R_{max}(n,n+p)} X(R) \cdot \exp\left[-\frac{U_2(R)}{kT_a}\right] \frac{R^4 \cdot dR}{a_0^5}, \quad (7)$$

where $g_{n;n+p}$ is Gaunt's factor for $|n\rangle \rightarrow |n+p\rangle$ transition, determined in [37]. The lower and upper bounds $R_{min}(n, n+p)$ and $R_{max}(n, n+p)$ are found as roots of the equations

$$U_{12}(R = R_{min}) = \epsilon_{n+p+1-\Delta p} - \epsilon_n, \quad U_{12}(R = R_{max}) = \epsilon_{n+p-\Delta p} - \epsilon_n \quad (8)$$

with $\epsilon_n = -Ry/n^2$ and $\Delta p = 0.380$. A factor $X(R)$ is given by

$$X(R) = \frac{\Gamma\left(\frac{3}{2}, \frac{-U_1(R)}{kT_a}\right)}{\Gamma\left(\frac{3}{2}\right)}, \quad (9)$$

and $\Gamma(x, y)$ and $\Gamma(x)$ are incomplete and complete gamma functions [38].

The deexcitation rate coefficients $K_{n-p;n}(T_a)$ are calculated from the thermodynamic balance equation in the case of helium plasma in the state of thermodynamical equilibrium with $T = T_a$, namely

$$K_{n-p;n}(T = T_a)N_{eq}(n-p)N_{eq}(1) = K_{n;n-p}(T = T_a)N_{eq}(n)N_{eq}(1), \quad (10)$$

where $N_{eq}(1)$, $N_{eq}(n-p)$ and $N_{eq}(n)$ are the corresponding equilibrium densities of the atoms $He(1s^2)$, $He^*(n-p)$ and $He^*(n)$, respectively. These densities satisfy equations

$$\begin{aligned} N_{eq}(n-p) &= N_{eq}(1) \cdot 4(n-p)^2 \exp\left(-\frac{I_{He} + \epsilon_{n-p}}{kT_a}\right), \\ N_{eq}(n) &= N_{eq}(1) \cdot 4n^2 \exp\left(-\frac{I_{He} + \epsilon_n}{kT_a}\right), \end{aligned} \quad (11)$$

where I_{He} is the ionization potential of $He(1s^2)$ atom. Consequently, the relation which links the excitation and deexcitation rate coefficients is

$$K_{n;n-p}(T_a) = K_{n-p;n}(T_a) \cdot \frac{(n-p)^2}{n^2} \cdot \exp\left(\frac{\epsilon_{n-p;n}}{kT_a}\right), \quad (12)$$

where $\epsilon_{n-p;n} = \epsilon_n - \epsilon_{n-p}$. The usage of the thermodynamical balance principle understands that in the equilibrium helium plasma with $T = T_a$ Boltzmann's distribution of helium excited atom populations has its full physical sense. One can directly confirm itself that this is valid for $T_a \gtrsim 3000K$. Because of that the described procedure can be certainly applied in the temperature region considered here.

3 Results and discussion

Equations (7)-(9) are used for rate coefficients $K_{n;n+p}(T_a)$ calculations. The results for $4 \leq n \leq 10$, $1 \leq p \leq 5$ and $4000K \leq T_a \leq 20000K$ are presented in Tab. 2. The Table shows a monotonous decrease of $K_{n;n+p}(T_a)$ with the increases of n and p , and a very slow increase as T_a increases. It should be noted that the differences between $K_{n;n+p}$ values for hydrogen from [10] and these for helium are caused by differences between the resonant distances $R_{n;n+p}$. The deexcitation rate coefficients $K_{n;n-p}(T_a)$ for $4 < n \leq 10$ and $4 \leq n - p$ are calculated according to Eq. (12) and using the values for excitation rate coefficient from Tab. 2.

The relative efficiency of $(n - n')$ -mixing processes (1) and (2) in comparison with electron-atom collision processes (3) is characterized by the quantity $F_{n;n\pm p}(T_a, T_e)$

$$F_{n;n\pm p}(T_a, T_e) = \frac{K_{n;n\pm p}(T_a)N(n)N(1)}{\alpha_{n;n\pm p}(T_e)N(n)N_e} = \frac{K_{n;n\pm p}(T_a)}{\alpha_{n;n\pm p}(T_e)} \cdot \eta_{ea}, \quad (13)$$

$$\eta_{ea} = \frac{N(1)}{N_e}, \quad (14)$$

where $\alpha_{n;n\pm p}(T_e)$ are the rate coefficients for the electron-atom excitation processes (3), and N_e is the free electron density. In the case of weakly ionized helium plasma the parameter η is closed to $(\text{ionization degree})^{-1}$. The values for $\alpha_{n;n\pm p}(T_e)$ are obtained from [39, 40].

The quantities $F_{n;n\pm p}(T_a, T_e)$ as functions of n for given p , T_a and T_e are illustrated in Figs. 3-9. They show that the efficiency of $(n - n')$ -mixing processes in $He^*(n) + He$ collisions, in domains $4 \leq n \leq 8$ and $n + 1 \leq n' \leq n + 5$, is higher or at least comparable to that of electron-atom processes (3), for all considered T_a and T_e .

The region $4 \leq n \leq 6$, where the minimum of helium excited atom populations' distribution occurs, is particularly important (see Fig. 1). In this domain the efficiency of processes (1) and (2) is significantly higher or very close to that of electron-atom processes (3). Such efficiency can explain the shape of distribution function, experimentally obtained in [12], and discussed in Sec. 1.

Regarding to the presented method accuracy we rely to the fact that $(n-n')$ -mixing processes are caused by the same resonant mechanism as the above mentioned chemi-ionization processes in symmetric atom-Rydberg atom collisions. Namely, these processes are well studied experimentally and theoretically and it was found that there is very good agreement between experimental and theoretical results [17–26].

The results of this paper suggest that the influence of the processes (1) and (2) on populating the lower part of Rydberg block of states has to be taken into account. It was shown in [32] that the similar mechanism in the chemi-ionization processes in weakly ionized hydrogen plasma, in region $4 \leq n \leq 8$, significantly changed the excited atom populations in the entire Rydberg block of states, and hence the changes in atomic spectral line shapes [41]. Therefore, the role of $(n - n')$ -mixing processes for the populations of the lower part of Rydberg block of states is of a special importance, the fact that has already been confirmed in the case of hydrogen [10].

The importance of chemi-ionization/recombination processes in weakly ionized helium plasmas has been confirmed earlier [30, 33], particularly when they were included within a model of collision radiative recombination [9]. On the other hands, the results presented here suggest a similar role for $(n - n')$ -mixing processes (1) and (2) in both helium and hydrogen plasmas. For example, these processes should influence helium spectral lines' shapes in cases of some helium rich white dwarfs atmospheres, in a research which already started [42]. They are also important for the kinetics of weakly ionized laboratory plasmas, which are always used in a research of gaseous discharges and inner-plasma collision processes [12, 43–48]. To conclude, the $(n - n')$ -mixing processes (1) and (2) have to be included in modeling of both laboratory and astrophysical weakly ionized helium plasmas.

References

- [1] Bates DR, Kingston AE, McWhirter RWP. Proc Roy Soc 1962;267:297
- [2] Bates DR, EKingston A. Proc Roy Soc 1964;279:32
- [3] Biberman LM, Vorobjev VS, Yakubov IT. Teplofizika vysokih temperatur 1967;5:201
- [4] Biberman LM, Vorobjev VS, Yakubov IT. Uspehi fiziceskih nauk 1979; 128:233
- [5] Vernazza J, Avrett E, Loser R. ApJS 1981;45:635
- [6] Maltby P, Avertt EH, Carlsson M, Kjeldseth-Moe O, Kurucz RL, Loeser R. ApJ 1986;306:284
- [7] Biberman LM, Vorobjev VS, Yakubov IT. Kinetics of Nonequilibrium Low-Temperature Plasma. Plenum, New York, 1987
- [8] Pert GJ. J Phys B 1990;23:619
- [9] Djurić Z, Mihajlov AA. JQSRT 2001;70:285
- [10] Mihajlov AA, Ignjatović LM, Djurić Z, Ljepojević NN. J Phys B 2004; 37:4493
- [11] Koester D. A&AS 1980;39:401
- [12] Aleksandrov VY, Gurevich DB, Podmoshenskii IV. Opt Spektrosk 1969; 36–41

- [13] Smirnov VM, Mihajlov AA. *Opt Spektrosk* 1971;30:984
- [14] Janev RK, Mihajlov AA. *Phys Rev A* 1979;20:1890
- [15] Mihajlov AA. In *Proc. of International Conference on Plasma Physics. G* 1982;
- [16] Devdariani AZ, Klyucharev AN, Lazarenko AB, Sheverev VA. *Pis'ma ZhTekhFiz* 1978;4:1013
- [17] Mihajlov AA, Janev RK. *J Phys B* 1981;14:1639
- [18] Weiner J, Polak-Dingels P. *J Chem Phys* 1981;74:508
- [19] Weiner J, Masnou-Seeuws F, Giusti-Suzor A. *Adv Atom Mol Opt Phys* 1989;26:209+
- [20] Klucharev AN, Vujnović V. *Physics Reports* 1990;185:55
- [21] Bezuglov NN, Borodin VM, Klyucharev AN, Fuso F, Allegrini M. *Optics and Spectroscopy* 1997;83:338
- [22] Bezuglov NN, Borodin VM, Kazanskiy AK, Klyucharev AN, Matveev AA, Orlovskiy KV. *Optics and Spectroscopy* 2001;91:19
- [23] Ryabtsev II, Tretyakov DB, Beterov II, Bezuglov NN, Miculis K, Ekers A. *J Phys B: At Mol Phys* 2005;38:S17
- [24] Beterov I, Tretyakov D, Ryabtsev I, Bezuglov N, Miculis K, Ekers A, Klucharev A. *J Phys B: Atom Molec Phys* 2005;38:4349
- [25] Miculis K, Beterov I, Bezuglov N, Ryabtsev I, Tretyakov D, Ekers A, Klucharev A. *J Phys B: At Mol Opt Phys* 2005;38:1811
- [26] Ignjatović L, Mihajlov AA. *Phys Rev A* 2005;72:022715
- [27] Janev RK, Mihajlov AA. *Phys Rev A* 1980;21:819
- [28] Mihajlov AA, Ljepojević NN, Dimitrijević MS. *J Phys B: At Mol Opt Phys* 1992;25:5121
- [29] Mihajlov AA, Dimitrijević MS, Djurić Z. *Physica Scripta* 1996;53:159
- [30] Mihajlov AA, Dimitrijević MS, Djurić Z, Ljepojević NN. *Physica Scripta* 1997;56:631
- [31] Mihajlov AA, Ignjatovic LM, Vasiljević MM, Dimitrijević MS. *Astronomy and Astrophysics* 1997;324:1206
- [32] Mihajlov AA, Jevremović D, Hauschildt P, Dimitrijević MS, Ignjatović LM, Alard F. *Astronomy and Astrophysics* 2003;403:787
- [33] Mihajlov AA, Ignjatović LM, Dimitrijević MS, Djurić Z. *The Astrophysical Journal Supplement Series* 2003;147:369
- [34] Mihajlov AA, Ignjatović LM, Dimitrijević MS. *Astronomy and Astrophysics* 2005;437:1023
- [35] Gupta BM, Madsen FA. *J Chem Phys* 1967;47:48
- [36] Metropoulos A, Li Y, Hirsch G, Buenker RJ. *Chemical Physics Letters* 1992;198:266
- [37] Johnson LC. *The Astrophysical Journal* 1972;174:227
- [38] Abramowitz M, Stegun IA. *Handbook of Mathematical Functions*. New York: Dover, 1965
- [39] Fujimoto T. *Institute of Plasma Physics, Nagoya, Japan, 1978*
- [40] Janev RK, Langer WD, Jr KE, Jr DEP. *Elementary Processes in Hydrogen-Helium Plasmas*. Springer-Verlag, 1987

- [41] Mihajlov AA, Jevremović D, Hauschildt P, Dimitrijević MS, Ignjatović LM, Alard F. *Astronomy and Astrophysics* 2007;In press
- [42] Beauchamp A, Wesemael F, Bergeron P. *The Astrophysical Journal Supplement Series* 1997;108:559
- [43] Aleksandrov VY, Gurevich DB, Mihajlov AA, Podmoshenskii IV. *Opt Spektrosk* 1974;37:855
- [44] Pendleton WR, Larsson M, Mannfors B. *Phys Rev A* 1985;28:3223
- [45] Kiselevskii LI, Mazurenko SL, Makarevich AN. *Proc ICPIA-18, Swansea* 1987;3:570
- [46] Bayarkhuu C, Kiselevskii LI, Mazurenko SL, Makarevich AN, Solov'yanchik DA. *Journal of Applied Spectroscopy* 1989;51:758
- [47] Solov'yanchik DA. *Journal of Applied Spectroscopy* 1993;59:340
- [48] Denkemann R, Maurmann S, Lokajczyk T, Drepper P, Kunze HJ. *J Phys B: At Mol Opt Phys* 1999;32:4635

Table 1
 $R_{n;n+p}/a_0$ values calculated from (5) for $n' = n + p$.

n	p				
	1	2	3	4	5
4	4.907	4.556	4.400	4.312	4.257
5	5.398	5.019	4.843	4.741	4.675
6	5.802	5.403	5.211	5.097	5.022
7	6.146	5.731	5.527	5.403	5.321
8	6.446	6.018	5.803	5.672	5.582
9	6.711	6.272	6.050	5.911	5.816
10	6.949	6.502	6.272	6.128	6.028

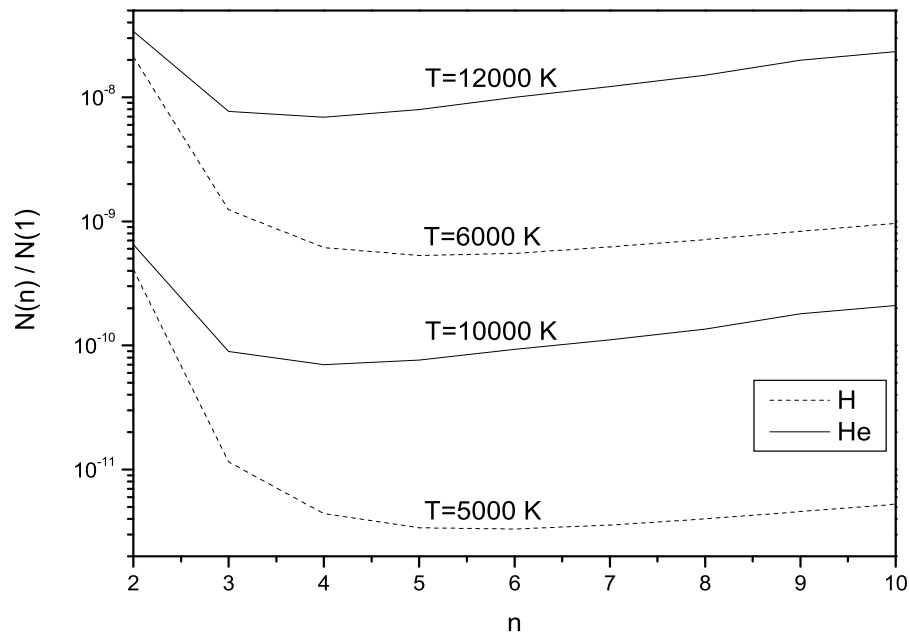


Fig. 1. The distribution function of excited atom population.

Table 2
Excitation rate coefficients $K_{n;n+p}(T_a)[10^{-9}cm^3s^{-1}]$.

n	p	$T_a[10^3 K]$									
		4.0	4.5	5.0	6.0	8.0	10.0	12.0	16.0	20.0	
1	1	1.005	1.080	1.143	1.243	1.378	1.462	1.520	1.594	1.638	
	2	0.195	0.221	0.244	0.283	0.338	0.374	0.400	0.434	0.455	
	4	3	0.072	0.084	0.095	0.114	0.142	0.161	0.175	0.194	0.206
		4	0.035	0.041	0.048	0.058	0.075	0.087	0.095	0.107	0.114
		5	0.020	0.024	0.028	0.035	0.045	0.053	0.058	0.066	0.071
2	1	0.682	0.707	0.728	0.760	0.800	0.824	0.841	0.861	0.873	
	2	0.170	0.182	0.191	0.207	0.227	0.239	0.248	0.258	0.265	
	5	3	0.072	0.078	0.083	0.092	0.103	0.111	0.116	0.122	0.126
		4	0.038	0.042	0.045	0.050	0.058	0.062	0.066	0.070	0.072
		5	0.023	0.025	0.027	0.031	0.036	0.039	0.041	0.044	0.046
3	1	0.432	0.441	0.448	0.459	0.473	0.481	0.486	0.493	0.497	
	2	0.124	0.128	0.132	0.138	0.146	0.151	0.154	0.157	0.160	
	6	3	0.056	0.059	0.062	0.065	0.070	0.073	0.075	0.077	0.079
		4	0.031	0.033	0.035	0.037	0.040	0.042	0.044	0.045	0.046
		5	0.019	0.021	0.022	0.024	0.026	0.027	0.028	0.029	0.030
4	1	0.276	0.279	0.282	0.286	0.292	0.295	0.297	0.299	0.301	
	2	0.086	0.088	0.089	0.092	0.095	0.097	0.098	0.100	0.101	
	7	3	0.041	0.042	0.044	0.045	0.047	0.049	0.049	0.050	0.051
		4	0.024	0.025	0.025	0.027	0.028	0.029	0.029	0.030	0.031
		5	0.015	0.016	0.016	0.017	0.018	0.019	0.019	0.020	0.020
5	1	0.181	0.183	0.184	0.186	0.188	0.189	0.190	0.191	0.192	
	2	0.059	0.060	0.061	0.062	0.064	0.065	0.065	0.066	0.066	
	8	3	0.030	0.030	0.031	0.032	0.033	0.033	0.034	0.034	0.034
		4	0.018	0.018	0.018	0.019	0.020	0.020	0.020	0.021	0.021
		5	0.011	0.012	0.012	0.013	0.013	0.013	0.014	0.014	0.014
6	1	0.122	0.123	0.124	0.125	0.126	0.126	0.127	0.127	0.128	
	2	0.042	0.042	0.043	0.043	0.044	0.044	0.045	0.045	0.045	
	9	3	0.021	0.022	0.022	0.022	0.023	0.023	0.023	0.024	0.024
		4	0.013	0.013	0.013	0.014	0.014	0.014	0.014	0.015	0.015
		5	0.009	0.009	0.009	0.009	0.009	0.010	0.010	0.010	0.010
7	1	0.085	0.086	0.086	0.086	0.087	0.087	0.087	0.088	0.088	
	2	0.030	0.030	0.031	0.031	0.031	0.031	0.032	0.032	0.032	
	10	3	0.016	0.016	0.016	0.016	0.017	0.017	0.017	0.017	0.017
		4	0.010	0.010	0.010	0.010	0.010	0.010	0.010	0.011	0.011
		5	0.006	0.007	0.007	0.007	0.007	0.007	0.007	0.007	0.007

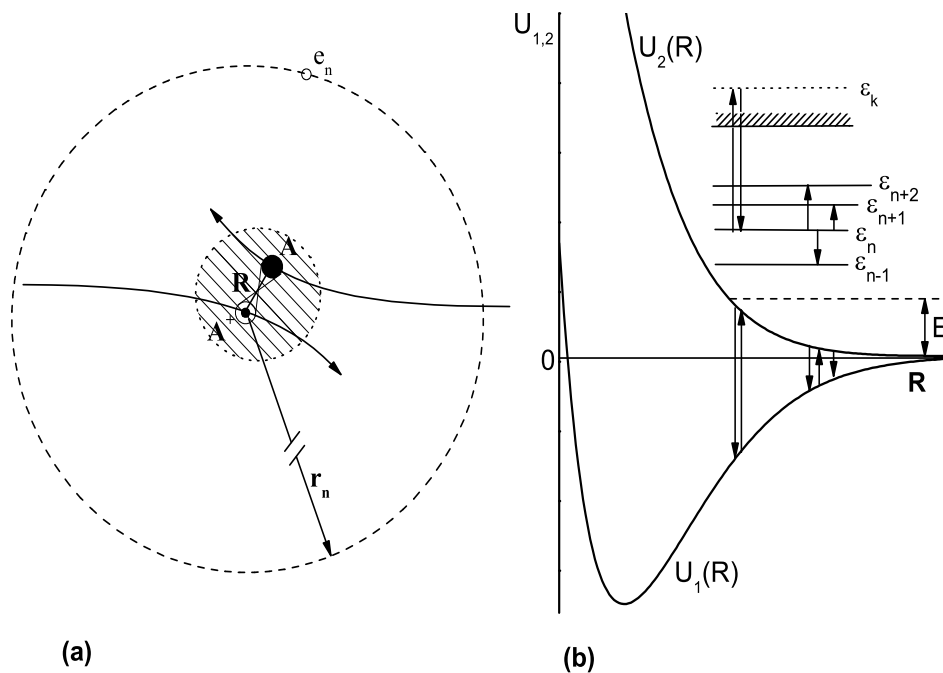


Fig. 2. (a) Schematic illustration of $He^*(n) + He$ collision (the region of the inter-nuclear distance R where the outer electron is collectivized is shaded); (b) Schematic illustration of the simultaneous resonant transitions of the outer electron from the initial bound to the final free state and the sub-system $He^+ + He$ from initial excited to the final ground electronic state.

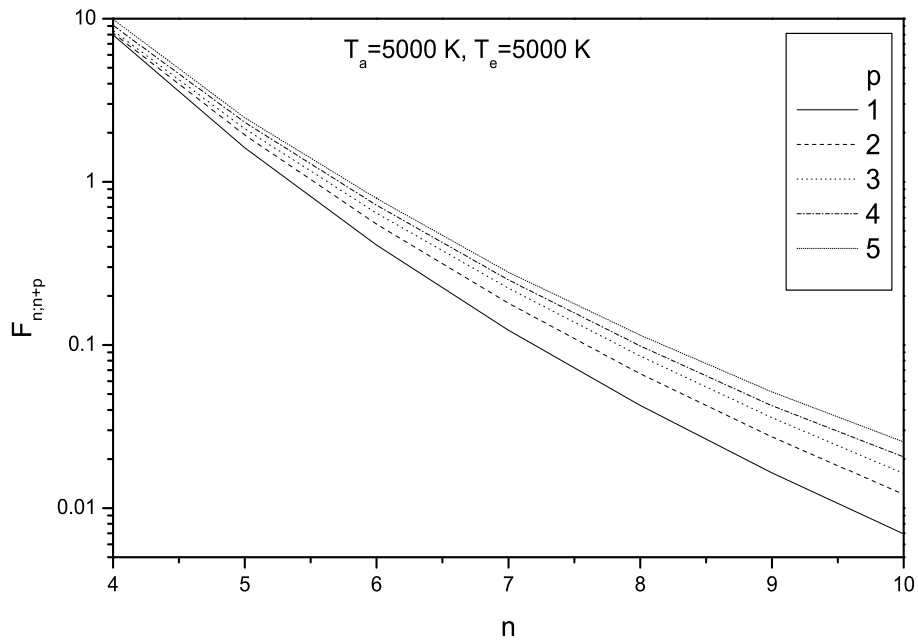


Fig. 3. Parameter $F_{n,n+p}$ for $T_a = 5000K$ and $T_e = 5000K$.

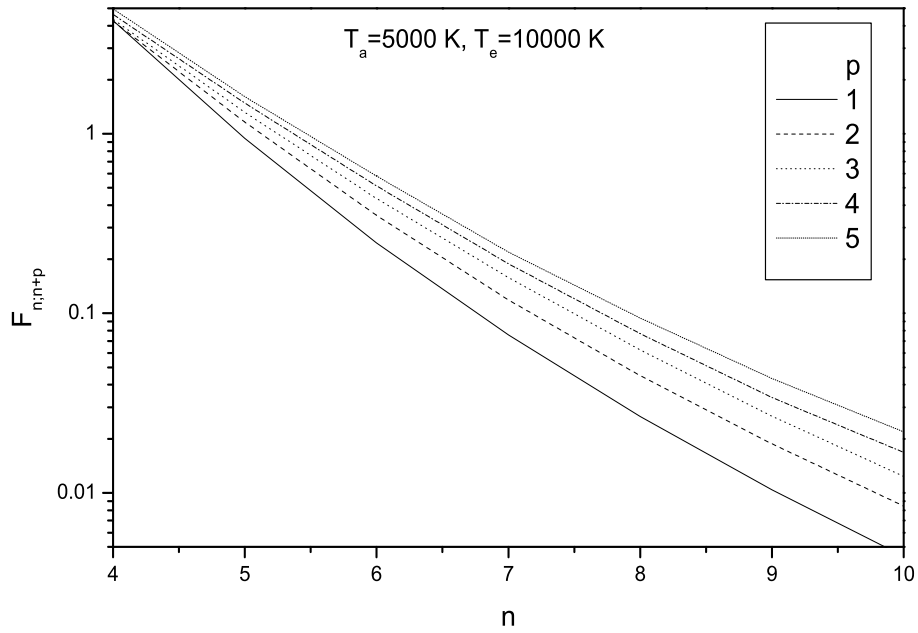


Fig. 4. Same as in Fig. 3, but for $T_a = 5000K$ and $T_e = 10000K$.

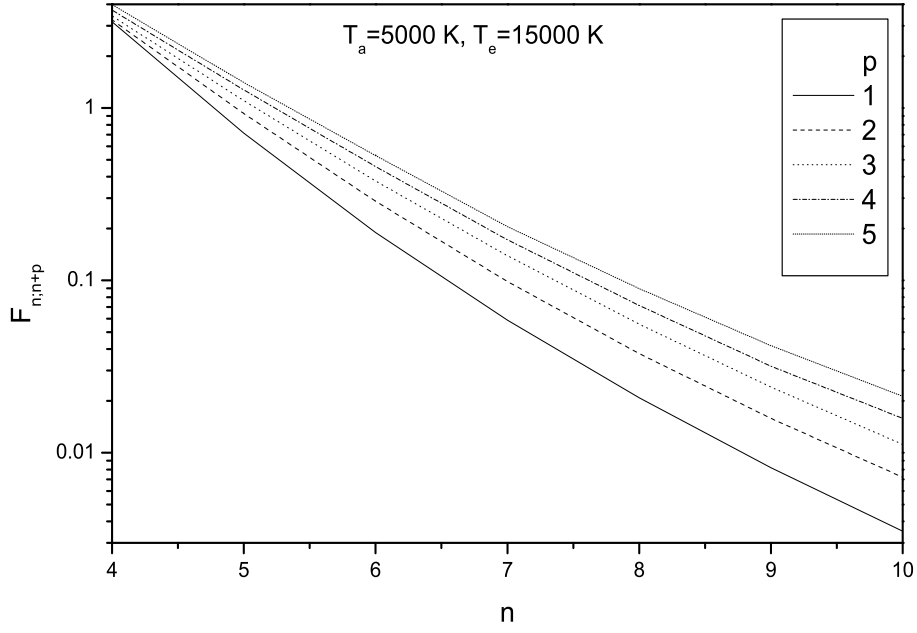


Fig. 5. Same as in Fig. 3, but for $T_a = 5000K$ and $T_e = 15000K$.

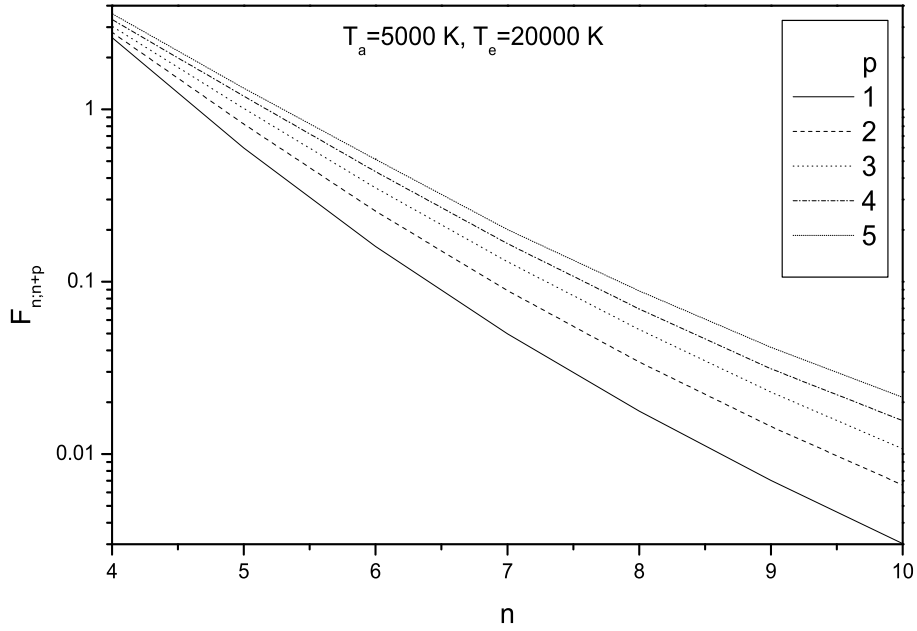


Fig. 6. same as in Fig. 3, but for $T_a = 5000K$ and $T_e = 20000K$.

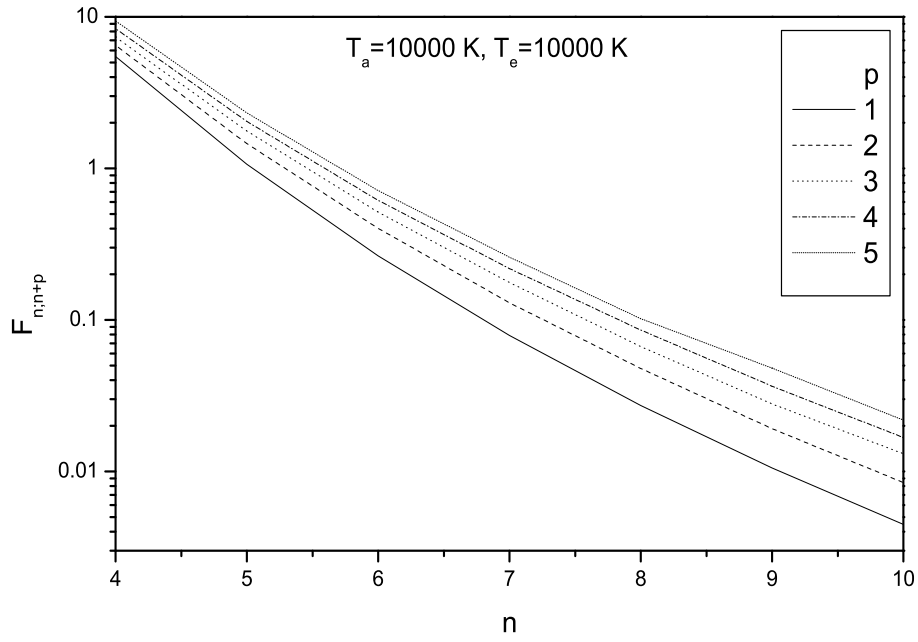


Fig. 7. Same as in Fig. 3, but for $T_a = 10000K$ and $T_e = 10000K$.

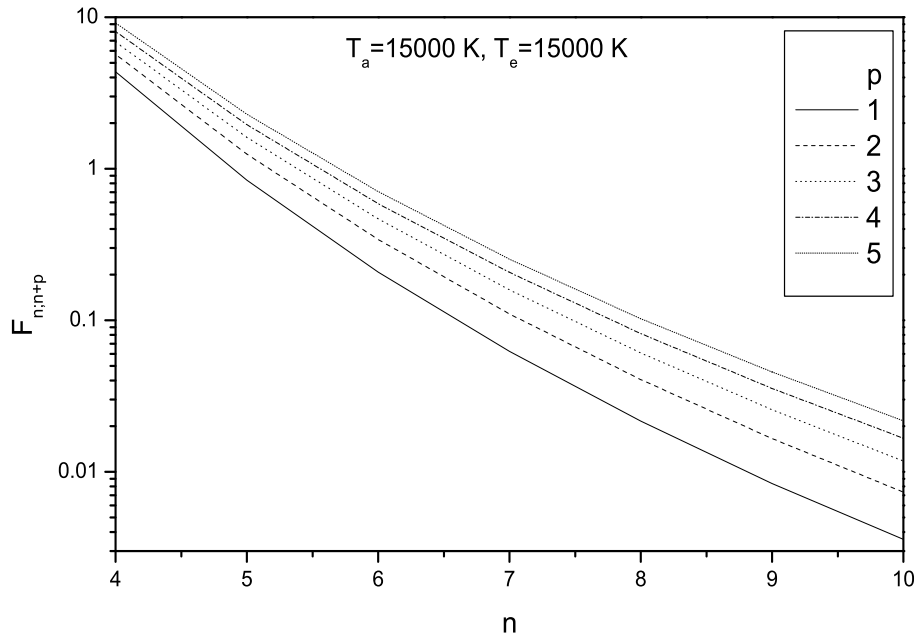


Fig. 8. Same as in Fig. 3, but for $T_a = 15000K$ and $T_e = 15000K$.

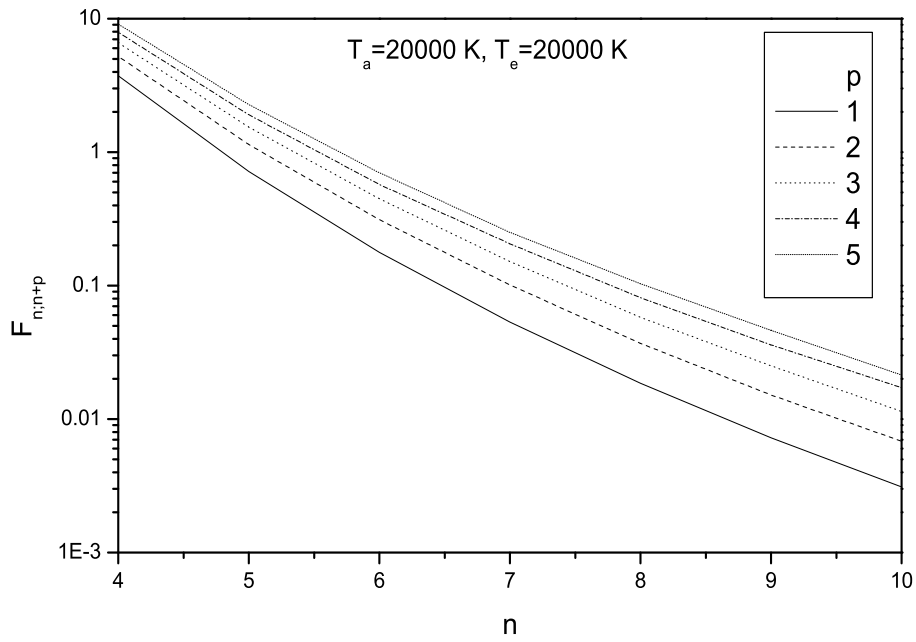


Fig. 9. Same as in Fig. 3, but for $T_a = 20000K$ and $T_e = 20000K$.